

# L-selectin mediated leukocyte tethering in shear flow is controlled by multiple contacts and cytoskeletal anchorage facilitating fast rebinding events

Ulrich S. Schwarz

*Theory Division, Max Planck Institute of Colloids and Interfaces, 14424 Potsdam, Germany*

Ronen Alon

*Department of Immunology, Weizmann Institute of Science, Rehovot, 76100 Israel*

L-selectin mediated tethers result in leukocyte rolling only above a threshold in shear. Here we present biophysical modeling based on recently published data from flow chamber experiments (Dwir et al., *J. Cell Biol.* 163: 649-659, 2003) which supports the interpretation that L-selectin mediated tethers below the shear threshold correspond to single L-selectin carbohydrate bonds dissociating on the time scale of milliseconds, whereas L-selectin mediated tethers above the shear threshold are stabilized by multiple bonds and fast rebinding of broken bonds, resulting in tether lifetimes on the timescale of  $10^{-1}$  seconds. Our calculations for cluster dissociation suggest that the single molecule rebinding rate is of the order of  $10^4$  Hz. A similar estimate results if increased tether dissociation for tail-truncated L-selectin mutants above the shear threshold is modeled as diffusive escape of single receptors from the rebinding region due to increased mobility. Using computer simulations, we show that our model yields first order dissociation kinetics and exponential dependence of tether dissociation rates on shear stress. Our results suggest that multiple contacts, cytoskeletal anchorage of L-selectin and local rebinding of ligand play important roles in L-selectin tether stabilization and progression of tethers into persistent rolling on endothelial surfaces.

## Introduction

Leukocyte trafficking plays a central role in the immune response of vertebrates. Leukocytes constantly circulate in the cardiovascular system and enter into tissue and lymph through a multi-step process involving rolling on the endothelium, activation by chemokines, arrest, and transendothelial migration [1]. A key molecule in this process is L-selectin, a leukocyte-expressed adhesion receptor which is localized to tips of microvilli and binds to glycosylated ligands on the endothelium. Its properties are optimized for initial capture and rolling under physiological shear [2, 3], as confirmed by recent experimental data and computer simulations [4, 5]. In contrast to tethering through other receptor systems like P-selectin, E-selectin or integrins, appreciable tethering through L-selectin and subsequent rolling only occurs above a threshold in shear [6], even in cell-free systems [7, 8]. Downregulation by low shear is unique for L-selectin tethers and might be necessary because L-selectin ligands are constitutively expressed on circulating leukocytes, platelets and subsets of blood vessels [9].

The dissociation rate of single molecular bonds is expected to depend exponentially on an externally applied steady force (*Bell equation*) [10]. Quantitative analysis with regular video camera (time resolution of 30 ms) of L-selectin tether kinetics in flow chambers above the shear threshold resulted in first-order dissociation kinetics, with a force dependence which could be fit well to the Bell equation, resulting in a force-free dissociation constant of 6.6 Hz [2, 3, 4, 11]. These findings have been interpreted as signatures of single L-selectin carbohydrate bonds. However, recent experimental evidence suggests that L-selectin tether stabilization involves multiple

bonds and local rebinding events. Evans and coworkers used the biomembrane force probe to measure unbinding rates for single L-selectin bonds as a function of loading force [12]. Modeling bond rupture as thermally activated escape over a sequence of transition state barriers increasingly lowered by rising force [13], these experiments revealed two energy barriers along the unbinding pathway. The inner barrier corresponds to  $\text{Ca}^{2+}$ -dependent binding through the lectin domain and explains the high strength of L-selectin mediated tethers required for cell capture from shear flow. Extracting barrier properties from the dynamic force spectroscopy data allows to convert them into a plot of dissociation rate as a function of force. In this way, results from dynamic force spectroscopy and flow chamber experiments can be compared in a way which is independent of loading rate. In detail, Evans and coworkers found a 1000-fold increase in dissociation rate as force rises from 0 to 200 pN, in marked contrast to tether dissociation kinetics as measured in flow chamber experiments, which increases at most 10-fold over this range [2, 3]. Therefore additional stabilization has to be involved with leukocyte tethers mediated by L-selectin. Dwir and coworkers used flow chambers to study tethering of leukocytes transfected with tail-modified mutants of L-selectin [14]. They found that tether dissociation increases with increased tail truncation, possibly since tail truncation leads to decreased cytoskeletal anchorage and increased mobility. More recently, Dwir and coworkers found with high speed video camera (time resolution of 2 ms) that L-selectin tethers form even below the shear threshold at shear rate 40 Hz, albeit with a very fast dissociation rate of 250 Hz, undetectable with regular camera [15]. Thus the shear threshold results from insufficient tether stabilization at low shear. Using systematic changes in viscosity

(which changes shear stress, but not shear rate), Dvir and coworkers were able to show that at the shear threshold, tether lifetime is prolonged by a factor of 14 due to shear-mediated cell transport over L-selectin ligand. They suggested that sufficient transport might be needed for formation of additional bonds. With more than one bond being present, rebinding then could provide the tether stabilization observed experimentally.

In this paper, we present a theoretical model for the interplay between bond rupture, L-selectin mobility and ligand rebinding within small clusters of L-selectin bonds, which interprets the recent experimental results in a consistent and quantitative way. Traditionally, tether dissociation at low ligand density has been interpreted as single molecule rupture due to the observed first order dissociation kinetics and a shear dependence which can be fit well to the Bell equation. Here we demonstrate that the same features result for small clusters of multiple bonds with fast rebinding. Our results suggest that the shear threshold corresponds to the formation of multiple contacts and that single L-selectin bonds decay too rapidly as to provide functional leukocyte tethers.

### Experiments

Our experimental procedures have been described before elsewhere [14, 15]. Three variants of human L-selectin were stably expressed in the mouse 300.19 pre B cell line. Wildtype, tail-truncated mutant and tail-deleted mutant have the same extracellular domains and differ only in their cytoplasmic tails. L-selectin mediated tethering was investigated in a parallel plate flow chamber. The main ligand used was PNAd, the major L-selectin glycoprotein ligand expressed on endothelium. For immobilization in the flow chamber, the ligand was diluted in such a way that no rolling was supported at shear rates lower than 100 Hz (dilution 10 ng/ml in the coating solution, which corresponds to an approximate scaffold density of  $100/\mu\text{m}^2$ ). Single tethers were monitored with video microscopy at 2 ms resolution and the microkinetics were analyzed by single cell tracking as described previously. The logarithm of the number of cells which pause longer than time  $t$  is plotted as a function of  $t$  and usually gives a straight line indicative of an effectively first order dissociation process. The slope is the tether dissociation rate  $k_{off}$  and is plotted as a function of shear rate  $\dot{\gamma}$  in Fig. 1. This plot shows that below the shear threshold of 40 Hz, the dissociation rate is 250 Hz, independent of tail mutations and viscosity of the medium. Above the shear threshold, the dissociation rate becomes force-dependent, with a dependence on shear stress which can be fit well to the Bell equation  $k_{off} = k_0 e^{F/F_b}$  [10]. Here  $k_0$  is the force-free dissociation rate and  $F_b$  is the bond's internal force scale. The force on an undeformed 300.19 lymphocyte with radius  $R = 6 \mu\text{m}$  follows from Stokes flow around a sphere close to a wall [16]. Taking into account the lever arm geometry

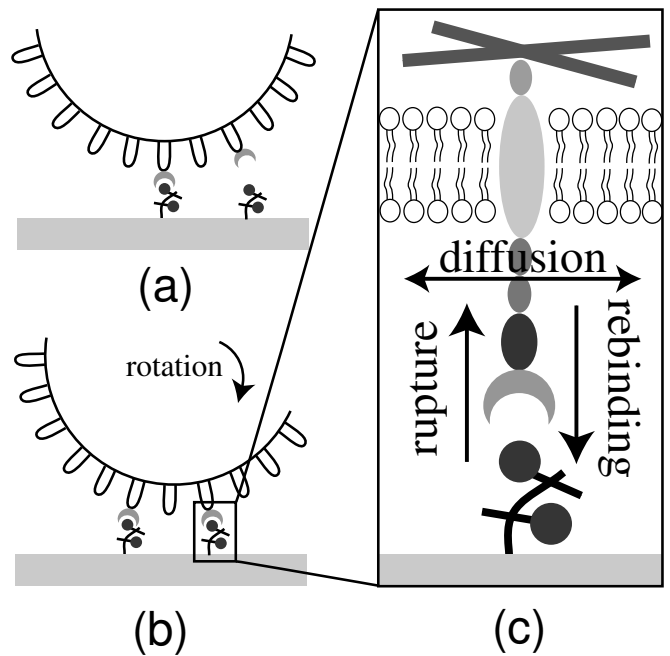


FIG. 1: Tether dissociation rate  $k_{off}$  determined from kinetic analysis of flow chamber experiments plotted as function of shear rate  $\dot{\gamma}$  [15]. Solid line with circles: wildtype. Dashed line with diamonds: tail-deleted mutant. Dotted line with squares: wildtype with 6 percent of Ficoll, which changes viscosity and thus shear stress (but not shear rate) by a factor of 2.6. These data suggest that the shear threshold is a transport-related rather than a force-related issue, and that the shear threshold is not about ligand recognition, but about tether stabilization.

provided by the tether holding the cell at an angle of  $50^\circ$ , the force acting on the L-selectin bonds can be calculated to be  $F = 180 \text{ pN}$  per  $\text{dyn}/\text{cm}^2$  of shear stress [3]. Fitting the Bell equation to the wildtype data from Fig. 1 gives similar values as obtained in earlier studies [2, 3, 4, 11], namely a force-free dissociation constant of 6.6 Hz and an internal force scale  $F_b = 200 \text{ pN}$  (corresponding to a reactive compliance of  $0.2 \text{ \AA}$ ). At the shear threshold, we find 14-fold and 7-fold reduction in dissociation rate for wildtype and tail-truncated mutant, respectively. Adding 6 volume percent of the non-toxic sugar Ficoll increases viscosity from 1 cP to 2.6 cP. Thus shear stress is increased by a factor of 2.6, whereas shear rate is unchanged. At the shear threshold, this increases wildtype dissociation 3-fold, roughly as expected from the fit to the Bell equation. Most importantly, there is no shift of the shear threshold as a function of shear rate. This indicates that the shear threshold results from shear-mediated transport, rather than from a force-dependent process.

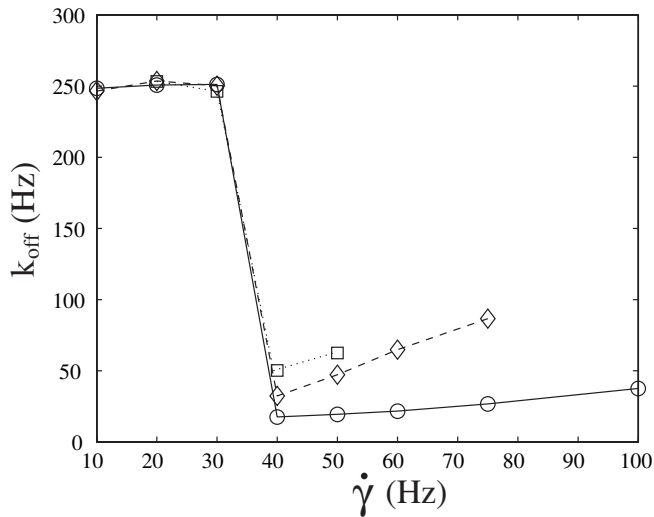


FIG. 2: A schematic representation of the mechanisms involved in L-selectin mediated leukocyte tethering to diluted carbohydrate ligands. (a) Initial binding most likely corresponds to one L-selectin receptor localized to the tip of one microvillus binding to ligand presented on a glycoprotein scaffold on the substrate. At low shear, stabilization through additional bonds is unlikely, because the distance between scaffolds is larger than the microvilli's tips and the probability of two microvilli simultaneously hitting two ligands is very low. (b) At sufficiently high shear, shear-mediated rotation of the cell over the substrate leads to the establishment of an additional bond on another microvillus. In contrast to this two-dimensional cartoon, in practice the two microvilli are expected to coexist with similar latitude, so that they can share force in a cooperative way. (c) Close-up to the cell-substrate interface. The L-selectin receptor can move laterally in the membrane, with an effective diffusion constant which depends on cytoskeletal anchorage. If a receptor has bound to ligand on the substrate, it will rupture in a stochastic manner, depending on shear-induced loading. If an additional bond (most likely on the second microvillus) holds the cell during times of rupture, rebinding can occur at the first microvillus, thus increasing tether stabilization.

### Theory

**Shear-mediated transport.** At the shear threshold at shear rate  $\dot{\gamma} = 40$  Hz (corresponding to shear stress  $\tau = \eta\dot{\gamma} = 0.4$  dyn/cm<sup>2</sup> for viscosity  $\eta = 1$  cP) and for small distance between cell and substrate, a cell with radius  $R = 6$   $\mu\text{m}$  will translate with hydrodynamic velocity  $u = 0.48R\dot{\gamma} = 0.12$   $\mu\text{m}/\text{ms}$  and at the same time rotate with frequency  $\Omega = 0.26\dot{\gamma} = 10.4$  Hz [16]. Therefore the cell surface and the substrate surface will move relatively to each other with an effective velocity  $v = u - R\Omega = 0.22R\dot{\gamma} = 50$  nm/ms. In average there is no normal force which pushes the cell onto the substrate, but since it moves in close vicinity to the substrate, it can explore it with this effective velocity  $v$ . Thus there exists a finite probability for a chance encounter between a

L-selectin receptors on the tip of a microvillus and a carbohydrate ligand on the substrate. Here we focus on the case of diluted ligands, with a ligand density of  $100/\mu\text{m}^2$ . Then the average distance between single ligands is 100 nm, that is larger than the lateral extension of the microvilli, which is 80 nm. Therefore the first tethering event is very likely to be a single molecular bond (compare Fig. 2a). If this first bond has formed, the microvillus will be pulled straight and the cell will slow down. It will come to a stop on the distance  $x$  of order  $\mu\text{m}$  (e.g. the rest length of a microvillus is  $0.35$   $\mu\text{m}$ ). This takes the typical time  $t_s = x/u = 8$  ms. During this time, the cell can explore an additional distance of the order of  $vt_s = 400$  nm. The experimental data presented in Fig. 1 suggest that this is the minimal transport required to establish a second microvillar contact which is able to contribute to tether stabilization (compare Fig. 2b).

**Single bond loading.** If tether duration was much longer than the time over which the cell comes to a stop, the single bond dissociation rate  $k_{off}$  below the shear threshold should increase exponentially with shear rate  $\dot{\gamma}$  according to the Bell equation. However, this assumption is not valid in our case, because tether duration and slowing down time are both in the millisecond range. Fig. 3 shows that indeed the Bell equation (dotted line) does not describe the wildtype data from Fig. 1 (dashed line with circles). In order to model a realistic loading protocol, we assume that the force on the bond rises linear until time  $t_s$  and then plateaus at the constant force  $F$  arising from shear flow. Note that initial loading rate  $r = F/t_s$  scales quadratically with shear rate  $\dot{\gamma}$ , because  $F \sim \dot{\gamma}$  and  $t_s \sim 1/\dot{\gamma}$ . The dissociation rate  $k_{off}$  for this situation can be calculated exactly. The result is given in the supplemental material and is plotted as dash-dotted line in Fig. 3. It is considerably reduced towards the experimentally observed plateau. Agreement is expected to increase further if initial loading is assumed to be sub-linear. A scaling argument shows the main mechanism at work. For the case of pure linear loading, the mean time to rupture is  $T = (F_b/r) \exp(k_0 F_b/r) E(k_0 F_b/r)$ , where  $E(x)$  is the exponential integral [17]. There are two different scaling regimes for slow and fast loading, which are separated by the critical loading rate  $r_c = k_0 F_b$ . For slow loading,  $r < r_c$ , a large argument expansion gives  $T \approx 1/k_0$ , that is the bond decays by itself before it starts to feel the effect of force. For fast loading, a small argument expansion gives  $T \approx (F_b/r) \ln(r/k_0 F_b)$ , which is also found for the most frequent time of rupture in this regime [13]. In our case,  $k_0 = 250$  Hz,  $F_b = 200$  pN and  $r_c = k_0 F_b = 5 \times 10^4$  pN/s. At the shear threshold,  $r = 10^4$  pN/s and we are still in the regime of slow loading,  $r < r_c$ . This suggests that tethers below the shear threshold correspond to single L-selectin carbohydrate bonds which decay before the effect of force becomes appreciable. This does not imply that the bonds do not feel any force (after all the cell is slowed down), but that we are in a regime in which  $k_{off}$  as a function of shear does not change appreciably, as observed experimentally.

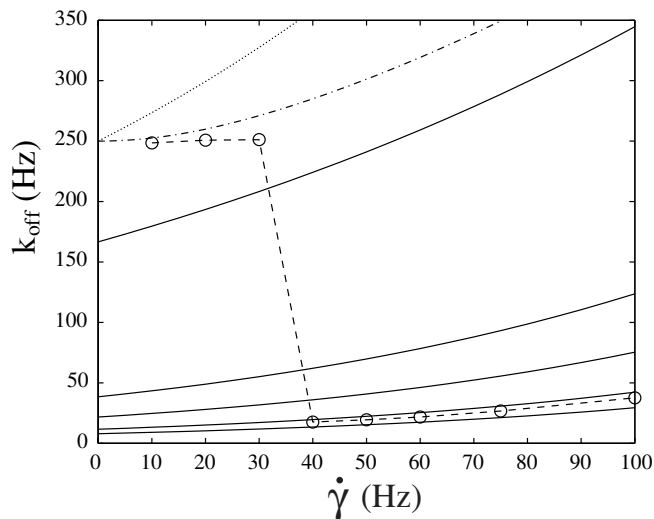


FIG. 3: Theoretical predictions for tether dissociation rate  $k_{off}$  as a function of shear rate  $\dot{\gamma}$  compared to experimentally measured wildtype data from Fig. 1 (dashed line with circles). Dotted line: the single bond dissociation rate with force-free dissociation rate  $k_0 = 250$  Hz and constant instantaneous loading increases exponentially according to the Bell equation. Dash-dotted line: it is reduced towards the experimentally observed plateau below the shear threshold at  $\dot{\gamma} = 40$  Hz by including the effect of finite loading rates. Solid lines from top to bottom: cluster dissociation rate for two-bonded tether with rebinding rate  $k_{on} = 0, 10, 20, 40$  and  $60 k_0$ . Above the shear threshold, the two-bonded tether with  $k_{on} \approx 10^4$  Hz agrees well with the experimentally measured data.

**Single bond rebinding.** Single bond rupture is a stochastic process according to the dissociation rate  $k_{off}$  given by the Bell equation. If ligand and receptor remain in spatial proximity after rupture, rebinding becomes possible. We define the single molecule rebinding rate  $k_{on}$  to be the rate for bond formation when receptor and ligand are in close proximity. If bond formation was decomposed into transport-determined formation of an encounter complex and chemical reaction of the two partners, then  $k_{on}$  would correspond to the on-rate for reaction [10, 18]. It has the dimension of 1/s and should not be confused with two- or three-dimensional association rates, which have dimensions of  $\text{m}^2/\text{s}$  (equivalently  $\text{m}/\text{Ms}$ ) and  $\text{m}^3/\text{s}$  (equivalently  $1/\text{Ms}$ ), respectively.  $k_{on}$  should depend mainly on the extracellular side of the receptor. In the following, it will therefore be assumed to be the same for wildtype and mutants. There are two mechanisms which might prevent rebinding within an initially formed cluster: the single receptor might escape from the rebinding region due to lateral mobility, or the receptor might be carried away from the ligand because the cell is carried away by shear flow. Fig. 2c shows schematically the interplay between rupture, rebinding and mobility for single L-selectin receptors.

We start with the first case, that is diminished re-

binding due to lateral receptor mobility. Since increased tail truncation decreases interaction with the cytoskeleton [19], lateral mobility increases from wildtype through tail-truncated to tail-deleted mutant. For each receptor type, we assume an effective diffusion constant  $D$ . The conditional probability for rebinding depends on absolute time since rupture. We approximate it by the probability that a particle with two-dimensional diffusion, but without capture is still within a disc with capture radius  $s$  at time  $t$ ,  $k_{on}(t) = k_{on}(1 - e^{-s^2/4Dt})$ . Thus the time scale for the diffusion correction is set by  $s^2/4D$ , the time to diffuse the distance of the capture radius. The diffusion constant for the wildtype can be estimated to be  $10^{-11} \text{ cm}^2/\text{s}$ , with the one for the tail-deleted mutant being at least one order of magnitude larger [20, 21]. A typical value for the capture radius is  $s = 1$  nm. Then the time  $t_c = s^2/4D$  to diffuse this distance is  $250 \mu\text{s}$  and  $25 \mu\text{s}$  for wildtype and tail-deleted mutant, respectively. For smaller times,  $t < t_c$ ,  $k_{on}$  plateaus at its initial value. For larger times,  $t > t_c$ , it decays rapidly towards zero. The single molecule behavior is governed by the dimensionless number  $k = k_{on}s^2/4D$ , which is the ratio of timescales set by diffusion and rebinding. Diffusion does not interfere with rebinding as long as  $k > 1$ . Our theory therefore predicts that for wildtype with diffusion constant  $D = 10^{-11} \text{ cm}^2/\text{s}$  and capture radius  $s = 1$  nm,  $k_{on} > 4 \times 10^3$  Hz. For the tail-deleted mutant, mobility does interfere with rebinding and we must have  $k < 1$ . If we assume that in this case  $D$  is smaller by one order of magnitude, then  $k_{on} < 4 \times 10^4$  Hz. Thus we can conclude that  $k_{on}$  should be of the order of  $10^4$  Hz.

#### Tether stabilization through multiple bonds.

We now turn to the possibility that spatial proximity required for rebinding is established by multiple contacts. Tethers above the shear threshold are modeled as clusters of  $N$  bonds, which in practice are expected to be distributed over at least two microvilli. At any time-point, each of the  $N$  bonds is either closed or open. The way force is shared between the closed bonds depends on the details of each tether realization. However, we expect that only those realizations will contribute significantly to the long-lived tethers above the shear threshold in which different bonds share force more or less equally. This most likely corresponds to two microvilli being bound with similar latitude in regard to the direction of shear flow. With this assumption, the force used in the single molecule dissociation rate has to be overall force divided by the number of closed bonds. If one bond ruptures, force is redistributed among the remaining bonds. Open bonds can rebind with the rebinding rate  $k_{on}$ . If rebinding occurs, force again is redistributed among the closed bonds. In general, in the absence of diffusion cluster lifetime  $T$ , but not the full cluster dissociation probability function can be calculated exactly [22]. We first discuss the case without loading or diffusion, thus focusing on the role of rebinding. As argued in the supplemental material, for small rebinding rate,  $k_{on} < k_0$ , cluster lifetime  $T$  scales logarithmically rather

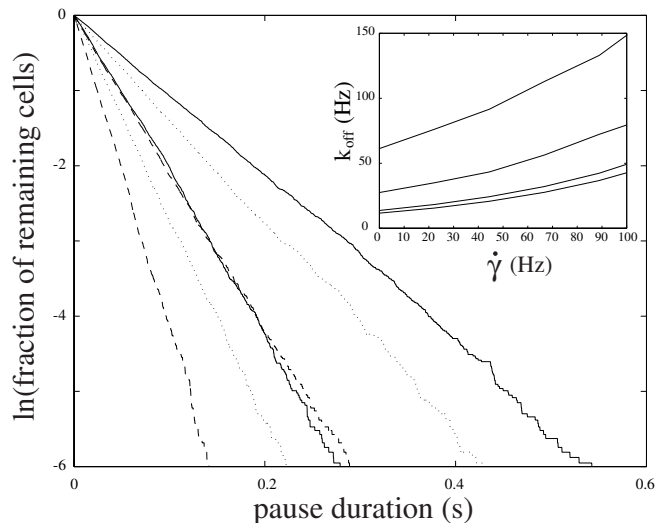


FIG. 4: Computer simulations show that L-selectin mediated tethers above the shear threshold yield first order dissociation kinetics. Solid lines: two-bonded tether with  $F = 0$  and  $k_{on} = 10^4$  (right) and  $0.5 \times 10^4$  Hz (left). Dashed lines: the same with  $F = 100$  pN. Dotted lines:  $k_{on} = 10^4$ ,  $F = 0$  and mobility parameter  $k = k_{on}s^2/4D = 1$  (right) and  $0.5$  (left), respectively. Inset: L-selectin mediated tethers show Bell-like shear dependence even in the presence of L-selectin mobility. Solid lines from bottom to top: no mobility,  $k = 2.5, 1$  and  $0.5$ .

than linear with cluster lifetime  $N$ . This weak increase in  $T$  with  $N$  results because different bonds decay not one after the other, but on the same time scale. The exact treatment shows that for clusters of 2, 10, 100, 1000 and 10,000 bonds without rebinding, lifetime is prolonged by 1.5, 2.9, 5.2, 7.5 and 9.8, respectively. In order to achieve 14-fold stabilization as observed experimentally at the shear threshold, one needs the astronomical number of  $6 \times 10^5$  bonds. In practice, for the case of dilute ligand discussed here, only very few bonds are likely. Therefore even in the presence of multiple bonds, rebinding is essential to provide tether stabilization.

In general, fast rebinding is much more efficient for tether stabilization than large cluster size. Our calculations predict that in order to obtain 14-fold stabilization for the cases  $N = 2, 3$  and  $4$ , one needs  $k_{on} = 6 \times 10^3, 10^3$  and  $550$  Hz, respectively. The value  $k_{on} = 6 \times 10^3$  Hz obtained for the case  $N = 2$  is surprisingly close to the estimate  $k_{on} = 10^4$  Hz obtained above via a completely different route, namely the competition of rebinding and diffusion for a single molecule. Therefore in the following we restrict ourselves to the simple case of two bonds being formed above the shear threshold (most probably by two microvilli). In this case, cluster lifetime can be calculated to be [22]:

$$T = \frac{1}{2k_0} \left( e^{-F/2F_b} + 2e^{-F/F_b} + \frac{k_{on}}{k_0} e^{-3F/2F_b} \right). \quad (1)$$

A derivation of this result is given in the supplemental material. In Fig. 3 we use Eq. (1) to plot the dissociation rate for the two-bonded tether (identified with the inverse of cluster lifetime  $T$ ) as a function of shear rate for different values of rebinding. The shear threshold at 40 Hz corresponds to  $F = 0.36 F_b$ . It follows from Eq. (1) that for this value of  $F$ , 14-fold stabilization in comparison with the force-free single bond lifetime is achieved for  $k_{on} \approx 44 k_0$ . For  $k_0 = 250$  Hz, this corresponds to a rebinding rate of  $k_{on} = 1.1 \times 10^4$  Hz. Thus again we arrive at the same order of magnitude estimate,  $k_{on} = 10^4$  Hz. Fig. 3 shows that with this value for  $k_{on}$ , agreement between theory and experimental wild-type data above the shear threshold is surprisingly good.

**Relation to BIAcore.** We now discuss how our estimate relates to BIAcore data for L-selectin [23]. In this experiment, L-selectin was free in solution and GlyCAM-1 immobilized on the sensor surface, which makes it a monovalent ligand. For the equilibrium dissociation constant, the authors found  $K_D = 105 \mu\text{M}$ . This unusually low affinity results from a very large dissociation rate  $k_r$ , which they estimated to be  $k_r \gtrsim 10$  Hz. The results presented in Fig. 1 seem to suggest that the real dissociation rate  $k_r = 250$  Hz. However, surface anchorage of both counter-receptors often reduces bond lifetime by up to two orders of magnitude [24]. This has been demonstrated experimentally for several receptor-ligand systems and might result from the reduction in free enthalpy of the anchored bond. Thus it might well be that the dissociation rate  $k_0 = 250$  Hz found for surface anchored bonds might be reduced down to  $k_r = 10$  Hz for free L-selectin binding to surface-bound ligand. Then the association rate  $k_f = 10^5$  1/Ms. For a capture radius  $s = 1$  nm and a three-dimensional diffusion constant  $D = 10^{-6}$  cm<sup>2</sup>/s, the diffusive forward rate in solution is  $k_+ = 4\pi Ds = 8 \times 10^8$  1/Ms. Because  $k_+ > k_f$ , the receptor-ligand binding in solution is reaction-limited, as it usually is. As explained above,  $k_{on}$  can be identified with the rate with which an encounter complex transforms into the final product [10, 18]. Since bond formation is reaction-limited,  $k_{on} = k_f K_+ = 4 \times 10^4$  Hz, where  $K_+ = 3/4\pi s^3$  is the dissociation constant of diffusion. Thus this estimate agrees well with the two other estimates derived above.

### Computer simulations

In order to obtain effective dissociation rates in the presence of diffusion, one has to use computer simulations. For each parameter set of interest, we used Monte Carlo simulations to simulate 5,000 realizations according to the rates given above. More details are described in the supplemental material. In general, our simulations show that for strong rebinding, that is  $k_{on} > k_0$ , the effective dissociation kinetics of small clusters is first order. In Fig. 4, this is demonstrated for the case  $N = 2$ . The plot shows the logarithm of the simulated number of tethers

lasting longer than time  $t$  for different parameter values of interest. All curves are linear, even in the presence of mobility, and the slopes can be identified with the dissociation rates. For example,  $k_{on} = 10^4$  Hz and  $F = 100$  pN yields the same effective first order dissociation rate as  $k_{on} = 0.5 \times 10^4$  Hz and  $F = 0$ , thus rebinding can rescue the effect of force. Our simulations also show that cluster dissociation rate as a function of force fits well to the Bell equation for  $k_{on} > k_0$ . In particular, this holds true in the presence of L-selectin mobility, as shown in the inset of Fig. 4. For  $k_{on} = 10^4$  Hz and without mobility (vanishing diffusion constant), lifetime at the shear threshold is 12-fold increased compared with single bond dissociation. With our estimate for wildtype mobility ( $k = k_{on}s^2/4D = 2.5$ ), 10-fold stabilization takes place. For tail-deleted mobility ( $k = 0.25$ ), only 1.5-fold stabilization occurs. This effect is more dramatic than observed experimentally, where stabilization for wildtype and tail-deleted mutant are 14-fold and 7-fold, respectively. In practice, the mobility scenario is certainly more complicated and is expected to smooth out the threshold effect arising from our modeling.

## Discussion

In this paper, we have presented biophysical modeling of L-selectin tether stabilization in shear flow based on recently published flow chamber data with high temporal resolution [15]. Our analysis suggests that the 14-fold stabilization observed at the shear threshold results from formation of multiple contacts and a single molecule rebinding rate of the order of  $k_{on} = 10^4$  Hz, which is remarkably faster than the force-independent dissociation rate  $k_0 = 250$  Hz observed below the shear threshold. Using computer simulations, we showed that for such strong rebinding, the experimentally observed first order dissociation and Bell-like shear force dependence follow from the statistics of small clusters of bonds. Despite the good quantitative agreement achieved here between experimental data and our model, it is important to state that it cannot be expected to predict all details of the experimental results. In practice, the formation of bonds is a stochastic process and there will be a statistical mixture of differently sized and differently loaded clusters, involving different microvilli and different scaffolds of L-selectin ligands. Cytoskeletal anchorage of the different ligand-occupied L-selectin molecules might also change in time in a complex way. Nevertheless, by focusing on the case of two bonds (possibly on two different microvilli) with shared loading and mobility-dependent rebinding, we obtained quantitative explanations for many conflicting observations from flow chamber experiments and biomembrane force probes, which have not been interpreted in a consistent way before.

Several explanations have been proposed for the shear threshold effect before. Chang and Hammer suggested that faster transport leads to increased probability for re-

ceptor ligand encounter [25]. Yet the new high resolution data from flow chamber experiments indicate that below the shear threshold, the issue is insufficient stabilization rather than insufficient ligand recognition [15]. Chen and Springer suggested that increased shear helps to overcome a repulsive barrier, possibly resulting from negative charges on the mucin-like L-selectin ligands [4]. However, Dwir and coworkers showed that small oligopeptide ligands for L-selectin presented on non-mucin avidin scaffolds exhibit the same shear dependence as their mucin counterparts [15]. Evans and coworkers have argued that increased shear leads to cell flattening and bond formation [12]. However, Dwir and coworkers found that fixation of PSGL-1 presenting neutrophils does not change the properties of tethers formed on low density immobilized L-selectin, while they do destabilize PSGL-1 tethers to immobilized P-selectin (Dwir and Alon, unpublished data). These data suggest that cell deformation as well as stretching and bending of microvilli do not play any significant role in L-selectin tether stabilization. Recently, the unusual molecular property of catch bonding has been suggested as explanation for the shear threshold [26, 27]. However, the data by Dwir and coworkers suggests that force-related processes do not account for the shear threshold of L-selectin mediated tethering [15]. Our interpretation of the shear threshold as resulting from multiple bond formation is supported by experimental evidence that increased ligand density both rescues the diffusion defect and abolishes the shear threshold [15]. The diffusion defect can also be rescued by anchoring of cell-free tail mutants of L-selectin to surfaces, allowing them to interact with leukocytes expressing L-selectin ligands [14].

On all ligands tested, the tail-truncated and more so the tail-deleted L-selectin mutants support considerably shorter tethers, consistent with a role for anchorage in these local stabilization events. One possible explanation is that cytoskeletal anchorage prevents uprooting of L-selectin from the cell. However, uprooting from the plasma membrane of neutrophils has been shown to take place on the timescale of seconds [28]. The tail-truncated L-selectin mutant has still two charged residues in the tail, which makes it impossible to extract it from the membrane in milliseconds. Receptor uprooting from the cytoskeleton only should lead to microvillus extension, which however is a slow process and has been shown to stabilize the longer-lived P-selectin mediated tethers rather than L-selectin mediated tethers [29]. Here we postulated another possibility for cytoskeletal regulation, namely restriction of lateral mobility. It has been argued before for integrin-mediated adhesion that increased receptor mobility due to unbinding from the cytoskeletal is used to upregulate cell adhesion [20, 21]. Indeed increased receptor mobility is favorable for contact *formation*, but here we show that it is unfavorable for contact *maintenance*, since it reduces the probability for rebinding.

Our analysis suggests that the smallest functional teth-



ers are mediated by a least two L-selectin bonds, each on a different microvillus, working cooperatively as one small cluster. Our model does not explain from which configuration a broken bond rebinds, but it suggests that this configuration is neither collapsed (otherwise rebinding, which implies spatial proximity, was not possible) nor strongly occupied (otherwise diffusive escape was not possible). We can only speculate that complete rupture is a multi-stage process, and that the rebinding discussed here starts from some partially ruptured state. We also cannot exclude that the rebinding events described here involve different partners than the dissociated ones, because both L-selectins and their carbohydrate ligands might be organized in a dimeric way. Moreover, cytoplasmic anchorage might proceed in multiple steps, including some weak pre-ligand binding anchorage, which is strengthened by L-selectin occupancy with ligand. Coupling between ligand binding and cytoplasmic anchorage is well-known for integrins [30] and might also be at work with selectins.

The mechanisms discussed in this paper could be effective also with other vascular counterreceptors specialized to operate under shear flow. As argued here, the exceptional capacity of L-selectin to promote functional adhesion in shear flow might not only result from fast dissociation and high strength under loading, but more so from a fast rebinding rate. Indeed other vascular adhesion receptors specialized to capture cells share on-rates similar to that of L-selectin [31]. Shear flow may also promote multi-contact formation for shear-promoted platelet tethering to von Willebrand factor [32]. It may also enhance formation of multivalent  $\alpha_4\beta_7$  and LFA-1 integrin tethers to their respective ligands [33, 34]. The importance of cytoskeletal anchorage in local rebinding processes of these and related adhesion receptors has not been experimentally demonstrated to date. However, the lesson drawn here from the role of L-selectin anchorage in millisecond tether stabilization may apply to these receptors as well. Future studies will help confirm this hypothesis. They will also shed light on the specialized structural features acquired by these receptors and their ligands through evolution, allowing them to operate under the versatile conditions of vascular shear flow.

**Acknowledgments:** We thank Oren Dwir, Thorsten Erdmann, Evan Evans, Stefan Klumpp, Rudolf Merkel, Samuel Safran and Udo Seifert for helpful discussions. R.A. is the Incumbent of The Tauro Career Development Chair in Biomedical Research. U.S.S. is supported by the German Science Foundation through the Emmy Noether Program.

### Supplemental material

**Model.** We consider a cluster with a constant number  $N$  of parallel bonds under constant force  $F$ . At any time  $t$ ,  $i$  bonds are closed and  $N - i$  bonds are open ( $0 \leq i \leq N$ ). Closed bonds are assumed to rupture according to

the Bell equation [10]:

$$k_{off} = k_0 e^{F/F_b} . \quad (2)$$

For convenience, we introduce dimensionless variables: dimensionless time  $\tau = k_0 t$ , dimensionless dissociation rate  $k_{off}/k_0$  and dimensionless force  $f = F/F_b$ . The  $i$  closed bonds are assumed to share force  $f$  equally, that is each closed bond is subject to the force  $f/i$ . Thus the dimensionless dissociation rate is  $e^{f/i}$ . As long as the receptors are held in proximity to the ligands, rebinding of open bonds can occur. Therefore we assume that single open bonds rebind with the force independent association rate  $k_{on}$ . The dimensionless rebinding rate is defined as  $\gamma = k_{on}/k_0$ .

The stochastic dynamics of the bond cluster can be described by a one-step Master equation [22]

$$\frac{dp_i}{d\tau} = r_{i+1}p_{i+1} + g_{i-1}p_{i-1} - [r_i + g_i]p_i \quad (3)$$

where  $p_i(\tau)$  is the probability that  $i$  closed bonds are present at time  $\tau$ . The reverse and forward rates between the different states  $i$  follow from the single molecule rates as

$$r_i = i e^{f/i} , \quad g_i = \gamma(N - i) . \quad (4)$$

Once the completely dissociated state  $i = 0$  is reached, the cell will be carried away by shear flow and the cluster cannot regain stability. This corresponds to an absorbing boundary at  $i = 0$ , which can be implemented by setting  $r_0 = g_0 = 0$ . Cluster lifetime  $T$  is identified with the mean time to reach the absorbing state  $i = 0$ .

**Lifetime of two bonded cluster.** For a cluster with two bonds,  $N = 2$ , cluster lifetime  $T$  can be calculated exactly in the following way. At  $\tau = 0$ , the cluster starts with the initial condition  $i = 2$ . Next it moves to state  $i = 1$  with probability 1, after the mean time  $1/r_2$ . From there, it rebinds to state  $i = 2$  with probability  $w_R = g_1/(r_1 + g_1)$ , or dissociates with probability  $w_D = r_1/(r_1 + g_1)$ . The mean time for this part is  $1/(r_1 + g_1)$ . Thus after two steps the system has reached state  $i = 0$  with probability  $w_D$  or returned to state  $i = 2$  with probability  $w_R$ , with  $w_D + w_R = 1$ . In detail, the probabilities and mean times for both processes are

$$w_D = \frac{e^f}{e^f + \gamma}, \quad t_D = \frac{1}{2e^{f/2}} + \frac{1}{e^f + \gamma}, \quad (5)$$

$$w_R = \frac{\gamma}{e^f + \gamma}, \quad t_R = t_D . \quad (6)$$

Different paths to dissociation only differ in the number of rebinding events  $j$  to state  $i = 2$ :

$$w_j = w_D w_R^j, \quad t_j = t_D + j t_R . \quad (7)$$

We first check normalization:

$$\sum_{j=0}^{\infty} w_j = w_D \frac{1}{1 - w_R} = 1 \quad (8)$$

and then calculate cluster lifetime:

$$T = \sum_{j=0}^{\infty} t_j w_j = t_D + t_R w_D \sum_{j=0}^{\infty} j w_R^j \quad (9)$$

$$= t_D + t_R w_D \frac{w_R}{(1-w_R)^2} = \frac{t_D}{1-w_R} \quad (10)$$

$$= \frac{1}{2} \left( e^{-f/2} + 2e^{-f} + \gamma e^{-3f/2} \right). \quad (11)$$

This formula is given in dimensional form as Eq. 1 in the main text.

**Cluster size versus rebinding.** For arbitrary cluster size  $N$ , cluster lifetime  $T$  can be obtained from the adjoint Master equation [22, 35]. In the case of vanishing force,  $f = 0$ , the solution can also be found by using Laplace transforms [22]:

$$T = \frac{1}{(1+\gamma)} \left( \sum_{i=1}^N \binom{N}{i} \frac{\gamma^i}{i} + \frac{1}{i} \right). \quad (12)$$

For  $\gamma = 0$ , this equation reduces to

$$T = \sum_{i=1}^N \frac{1}{i} = H_N \quad (13)$$

where  $H_N$  are the harmonic numbers. An expansion for large  $N$  gives

$$H_N = \Gamma + \ln N + \frac{1}{2N} + O\left(\frac{1}{N^2}\right). \quad (14)$$

Here  $\Gamma = 0.577$  is the Euler constant. This formula is rather good already for small values of  $N$ . Eq. (13) is easy to understand: for  $\gamma = 0$ , dissociation is simply a sequence of Poisson decays with mean times  $1/r_i = 1/i$ . The overall mean time for dissociation is the sum of the mean times of the subprocesses. We conclude that for vanishing rebinding,  $T$  grows only weakly (logarithmically) with  $N$  and very large cluster sizes are required to achieve long lifetimes [17, 36]. Therefore rebinding is essential to achieve stabilization for small cluster sizes.

**Effect of finite loading rate.** Loading and dissociation of single L-selectin bonds occur on the same time scale. As a cell is captured from shear flow and comes to a stop, force rises from zero and plateaus at a finite value. We model the initial rise as linear, with loading rate  $r$ . Therefore  $f = \mu\tau$  until time  $\tau_0$ , followed by constant loading  $f = f_0$ , where  $\mu = r/k_0 F_b$  is dimensionless loading rate. Since  $\mu = f_0/\tau_0$ , there are only two independent parameters,  $\tau_0$  and  $f_0$ . The mean lifetime can be calculated in the usual way [13, 17]. We find

$$T = \frac{e^{\frac{1}{\mu}}}{\mu} \left( E\left(\frac{1}{\mu}\right) - E\left(\frac{e^{\mu\tau_0}}{\mu}\right) + \frac{\mu}{e^{f_0}} e^{-\frac{e^{\mu\tau_0}}{\mu}} \right) \quad (15)$$

where  $E(x)$  is the exponential integral. For  $\tau_0 \rightarrow 0$ , we find the result for constant loading,  $T = 1/e^{f_0}$ . For  $\tau_0 \rightarrow \infty$ , we find the result for linear loading,  $T = e^{1/\mu} E(1/\mu)/\mu$  [17]. Eq. (15) is used in the section on single bond loading and for the plot of the dash-dotted line in Fig. 3.

**Simulations.** In the presence of diffusion with diffusion constant  $D$ , the single molecule association rate becomes a function of the time  $t$  which has passed since unbinding. In this paper, we use the approximation

$$k_{on}(t) = k_{on} \left( 1 - e^{-s^2/4Dt} \right) \quad (16)$$

where  $s$  is the capture radius. Since analytical solutions are intractable in this case, the Master equation Eq. (3) has to be solved numerically. The standard method to do so are Monte Carlo simulations. Unfortunately, the Gillespie algorithm for exact stochastic simulations [37] cannot be used in this case, because it does not track the identity of different bonds [38]. Therefore we simulate the Master equation by discretizing time  $\tau$  in small steps  $\Delta\tau$ . For each time step, random numbers are drawn in order to decide how the system evolves according to the rates defined for the different processes. In detail, in the time interval  $[\tau, \tau + \Delta\tau]$  each closed bond has the probability  $e^{f/i} \Delta\tau$  to rupture, and each open bond has the probability  $\gamma(1 - e^{-k/(\gamma\tau)}) \Delta\tau$  to rebind. Here  $k = k_{on} s^2/4D$  is the dimensionless ratio of the timescales set by diffusion and rebinding. Our model for stochastic cluster dynamics was implemented in the programming environment Matlab. A typical run simulates 5,000 tethers (larger tether numbers give better statistics for the long time behaviour, but similar results), each comprising  $N$  bonds. Results from different runs are binned into histograms for the number of tethers dissociating in the time interval  $[\tau, \tau + \Delta\tau]$ . In Fig. 4, we plot the natural logarithm of the fraction of tethers which last longer than dimensional time  $t$  as a function of  $t$ , as it is common for the analysis of experimental data. The slope of this curve is identified with the dissociation rate. Although this procedure involves numerical integration of the probability distribution for dissociation, and therefore leads to loss of information, its smoothing effect is essential to obtain reliable estimates for the dissociation rate in the presence of noisy data. In the inset of Fig. 4, the dissociation rates obtained in this way are plotted as function of shear rate (that is force) and diffusion constant (which determines the dimensionless parameter  $k$ ).



- ture **374**, 539–542.
- [3] Alon, R., Chen, S., Puri, K. D., Finger, E. B., & Springer, T. A. (1997) *J. Cell Biol.* **138**, 1169–1180.
- [4] Chen, S. & Springer, T. A. (1999) *J. Cell Biol.* **144**, 185–200.
- [5] Chang, K.-C., Tees, D. F. J., & Hammer, D. A. (2000) *Proc. Natl. Acad. Sci. USA* **97**, 11262–11267.
- [6] Finger, E. B., Puri, K. D., Alon, R., Lawrence, M. B., vonAndrian, U. H., & Springer, T. A. (1996) *Nature* **379**, 266–269.
- [7] Alon, R., Chen, S., Fuhlbrigge, R., Puri, K. D., & Springer, T. A. (1998) *Proc. Natl. Acad. Sci. USA* **95**, 11631–11636.
- [8] Greenberg, A. W., Brunk, D. K., & Hammer, D. A. (2000) *Biophys. J.* **79**, 2391–2402.
- [9] Kansas, G. S. (1996) *Blood* **88**, 3259–3287.
- [10] Bell, G. I. (1978) *Science* **200**, 618–627.
- [11] Chen, S. & Springer, T. A. (2001) *Proc. Natl. Acad. Sci. USA* **98**, 950–955.
- [12] Evans, E., Leung, A., Hammer, D., & Simon, S. (2001) *Proc. Natl. Acad. Sci. USA* **98**, 3784–3789.
- [13] Evans, E. & Ritchie, K. (1997) *Biophys. J.* **72**, 1541–1555.
- [14] Dwir, O., Kansas, G. S., & Alon, R. (2001) *J. Cell Biol.* **155**, 1–13.
- [15] Dwir, O., Solomon, A., Mangan, S., Kansas, G. S., Schwarz, U. S., & Alon, R. (2003) *J. Cell Biol.* **163**, 649–659.
- [16] Goldmann, A. J., Cox, R. G., & Brenner, H. (1967) *Chem. Eng. Sci.* **22**, 653–660.
- [17] Tees, D. F. J., Woodward, J. T., & Hammer, D. A. (2001) *J. Chem. Phys.* **114**, 7483–7496.
- [18] Shoup, D. & Szabo, A. (1982) *Biophys. J.* **40**, 33–39.
- [19] Pavalko, F. M., Walker, D. M., Graham, L., Goheen, M., Doerschuk, C. M., & Kansas, G. S. (1995) *J. Cell Biol.* **129**, 1155–1164.
- [20] Chan, P. Y., Lawrence, M. B., Dustin, M. L., Ferguson, L. M., Golan, D. E., & Springer, T. A. (1991) *J. Cell Biol.* **115**, 245–255.
- [21] Kucik, D. F., Dustin, M. L., Miller, J. M., & Brown, E. J. (1996) *J. Clin. Invest.* **97**, 2139–2144.
- [22] Erdmann, T. & Schwarz, U. S. (2004) *Phys. Rev. Lett.* **92**, 108102.
- [23] Nicholson, M. W., Barclay, A. N., Singer, M. S., Rosen, S. D., & van derMerwe, P. A. (1998) *J. Biol. Chem.* **273**, 763–770.
- [24] Nguyen-Duong, M., Koch, K. W., & Merkel, R. (2003) *Europhys. Lett.* **61**, 845–851.
- [25] Chang, K.-C. & Hammer, D. A. (1999) *Biophys. J.* **76**, 1280–1292.
- [26] Marshall, B. T., Long, M., Piper, J. W., Yago, T., McEver, R. P., & Zhu, C. (2003) *Nature* **423**, 190–193.
- [27] Sarangapani, K. K., Yago, T., Klopocki, A. K., Lawrence, M. B., Fieger, C. B., Rosen, S. D., McEver, R. P., & Zhu, C. (2004) *J. Biol. Chem.* **279**, 2291–2298.
- [28] Shao, J.-Y. & Hochmuth, R. M. (1999) *Biophys. J.* **77**, 587–596.
- [29] Yago, T., Leppänen, A., Qiu, H., Marcus, W. D., Nollert, M. U., Zhu, C., Cummings, R. D., & McEver, R. P. (2002) *J. Cell Biol.* **158**, 787–799.
- [30] Hynes, R. O. (2002) *Cell* **110**, 673–687.
- [31] van derMerwe, P. A. & Davis, S. J. (2003) *Annu. Rev. Immunol.* **21**, 659–84.
- [32] Doggett, T. A., Girdhar, G., Lawshe, A., Schmidtke, D. W., Laurenzi, I. J., Diamond, S. L., & Diacovo, T. G. (2002) *Biophys. J.* **83**, 194–205.
- [33] deChateau, M., Chen, S., Salas, A., & Springer, T. A. (2001) *Biochemistry* **40**, 13972–9.
- [34] Salas, A., Shimaoka, M., Chen, S., Carman, C. V., & Springer, T. (2002) *J. Biol. Chem.* **277**, 50255–62.
- [35] vanKampen, N. G. (1992) *Stochastic processes in physics and chemistry* (Elsevier, Amsterdam).
- [36] Goldstein, B. & Wofsy, C. (1996) *Immunology Today* **17**, 77–80.
- [37] Gillespie, D. T. (1977) *J. Phys. Chem.* **81**, 2340–2361.
- [38] Firth, C. A. J. M. & Bray, D. (2001) Stochastic simulation of cell signaling pathways, in *Computational modeling of genetic and biochemical networks*, eds. Bower, J. M. & Bolouri, H. (MIT, Boston), pp. 263–286.